Transactions on Engineering and Technology Research
ISSN: 2960-1797, eISSN: 2960-2246 | Volume 3
ICMEIT 2024

Phase field simulations of microstructure evolution of monocrystalline and polycrystalline silicon by forced convection

Dianxi Zhang [1,*], Xiufan Yang [1,a], Xinmao Qin [1,b], Huaizhi Wang [2,c] and Qingjiang Song [1,d]

[1]College of Physics and Electronic Science, Anshun University, Anshun 561000, China;

[2]School of Materials Science and Engineering, Qingdao University, Qingdao 266071, China;

[*]Correspondence: xiwa_315@163.com

[a]xnmdyxf@163.com; [b]qxm200711@126.com; [c]wanghuaizhilz@163.com, [d]18785760382@163.com;

Abstract. In this study, the phase field method was used to numerically simulate single crystal and polycrystalline silicon under the action of forced convection. Following the construction of the phase field model, the effects of parameters such as the degree of undercooling and convection velocity on the growth morphology of monocrystalline and polycrystalline silicon were simulated. The crystal nuclei of different sizes and multi-grain growth conditions of different nucleation times were obtained. The results showed that the growth rate of the upstream tip was the fastest, followed by that of the horizontal direction, and the growth rate of the lower end was the slowest under forced convection. When the undercooling degree was small, anisotropy was not obvious, and grain growth was slow. When the undercooling degree was greater than 0.65, the interface became unstable, and side branches appeared in the direction of the horizontal dendrite arm, while growth was transformed from the non-small crystal plane to the small crystal plane. Under the action of forced convection, the larger the flow velocity, the faster the crystal growth, and the faster the growth speed in the upstream direction of the grain. During the early growth stage, the overall growth rate of the larger initial nuclei was slower than that of the smaller initial nuclei, and subsequently, the difference was not significant. As the grains continued to grow, the thermal diffusion layers of the adjacent grains were in contact with each other, resulting in competitive growth.

Keywords: forced convection; Monocrystalline silicon; Polysilicon; nucleation.

1. Introduction

Research on the growth process of zoned silicon single crystal has been beneficial to obtain excellent semiconductor silicon materials. The crystallization process of zone-melted single crystal silicon is very complicated, with convection being an important factor. Sabanskis [1] used simulation software OpenFOAM to make a two-dimensional comparison of the atmosphere in the zone furnace, such as argon and helium gas, the gas flow under a vacuum, and the shape of the phase interface, and comprehensively compared the extra heat loss caused by the gas flow on the surface of the monocrystalline silicon rod. Han et al. [2] applied a fluid volume model to simulate the free surface shape of a three-dimensional model, which was consistent with the results obtained by previous researchers using a two-dimensional model. G. Ruatnieks et al. [3] numerically simulated the interface shape of the melting zone under metastable, semi-transient, and transient conditions. Michael et al. [4] found that the distribution of the electromagnetic field determined each interface and affected the flow of the fluid in the molten zone, where the flow of the fluid affected the distribution of the dopant concentration field in the molten zone. The presence of convection in the molten zone was an indisputable fact; however, the researchers did not study the effect of convection on the microstructure. Chen et al. [5] discussed the growth competition phenomenon, which agreed well with the experimental observations. Aoyama et al. [6] obtained a silicon dendrite morphology via large supercooling experiments. However, no simulations showing the key experimental features have been carried out so far. Granasy et al. [7,8] considered the phenomenon of nucleation, which

was successfully extended to model the solidification of highly anisotropic systems [9–11]. Kasajima et al. [11] applied a small solid/liquid interface limit to the phase field model to simulate the growth of small crystal face dendrites during the solidification of supercooled Si. The simulation results were similar to the Gibbs-Thomson relationship. Chen et al. [12] used the phase field method to simulate and calculate the evolution process of the dendrites on a facet of elemental silicon to obtain the influence law of the anisotropy coefficient on dendrite growth. Liu et al. [13] used a phase field model with high interfacial energy anisotropy to study the effect of interfacial energy anisotropy and undercooling on interfacial morphology during free growth of the silicon grains. Lin et al. [14] simulated the 3D phase field of directionally solidified silicon film growth. Several attempts have been made to simulate the dendritic growth of faceted materials [15–16]. Yuan et al. [17] simulated the evolution of interfacial morphology during polysilicon solidification by the phase-field method and analyzed the effects of initial nucleation conditions, disturbance intensity, and time step on interfacial morphology evolution. Du [18] found that the Boundary heat flux had a significant effect on the solidification behavior and microstructure formation, as it could directly affect the interfacial heat flux and cooling rate during phase transition. Chen [19] studied the growth of twin-related silicon dendrites using the novel phase-field model. The correctness of the model for an equilibrium twined crystal was examined first, before faceted dendrite growth was modeled. The simulated morphologies of 〈112〉 and 〈110〉 faceted dendrites were consistent with the experimental observations.

Convection will affect the morphology of crystalline microstructures. Although researchers have studied microstructures, they have not studied the evolution law of silicon crystal microstructures under the action of convection. The convective effect during solidification has an important influence on the growth mechanism of solid-liquid interface, as it can not only change the temperature distribution and temperature gradient but can also affect the nucleation mechanism, the distribution of solutes, and the growth of crystals. It may be particularly beneficial to simulate the microstructure evolution, for better application in production practice.

The theoretical analysis of nucleation time, number, distribution, and growth of crystal nuclei in the existing simulation must be further improved. As mentioned above, convection has been shown to play an important role in the crystal growth mechanism; therefore, further studies are needed to investigate the effect of convection on the microstructure evolution of silicon crystals.

In this study, using the proposed Tong[20] coupling flow field of the phase field model on the basis of correction, we considered the anisotropy of interfacial energy, using the fixed phase field model to simulate the crystal rotation generated when the forced convection across the cold silicon melted in the asymmetric growth behavior of the silicon crystal, and the simulation of crystal morphology was in good agreement with the theoretical analysis.

2. Phase Field Model

In the case of pure matter, a heat diffusion equation will also be incorporated along with the latent heat term:

$$\frac{\partial T}{\partial t} = D_T \nabla^2 T + h`(\varphi) \frac{L}{c_p} \frac{\partial \varphi}{\partial t} \tag{1}$$

where $D_T = K_T/c_p$ is the thermal diffusivity, L is the latent heat, and c_p is the specific heat capacity. Upon introducing the dimensionless temperature $u = (T - T_m)/(L/C_p)$, (1) will take the following form:

$$\frac{\partial u}{\partial t} = D_T \nabla^2 u + \frac{1}{2} \frac{\partial \varphi}{\partial t} \tag{2}$$

We considered the anisotropic phase field governing equation:

$$\tau_0 a_s(\theta')\frac{\partial \varphi}{\partial t} = [\varphi - \lambda u(1-\varphi^2)](1-\varphi^2)$$

$$+\varepsilon_0^2 \nabla \cdot (a_s(\theta')^2 \nabla\varphi) - \frac{\partial}{\partial x}\left(\varepsilon_0^2 a_s(\theta') a_s{}'(\theta')\frac{\partial}{\partial y}\right) + \frac{\partial}{\partial y}\left(\varepsilon_0^2 a_s(\theta') a_s{}'(\theta')\frac{\partial}{\partial x}\right) \quad (3)$$

where ϕ represents the phase field parameter, $\phi = 1$ represents the bulk solid phase, and $\phi = -1$ represents the bulk liquid phase. The phase field varied smoothly between these two values within the diffusion interface region, where $\lambda = 6.359$ [12].

Wulff studied equilibrium crystal shapes [12] at various anisotropy values. When $\gamma < 1/15$, the crystal shape was smooth and continuous, and when $\gamma > 1/15$, there were discontinuous and concave features similar to ears. These so-called ears increased with increasing anisotropy value. To simulate dendritic growth with strong anisotropy, these ears had to be removed. The interface energy within the missing orientations was normalized by Eggleston and Kim as follows:

$$\widehat{W}(\varphi) = \begin{cases} W(\varphi), (\frac{\pi}{2}i + \varphi_m) \le |\varphi| \le \frac{\pi}{2}(i+1) - \varphi_m \\ \frac{W(\varphi_m)\cos\varphi}{cos\varphi_m}, (\frac{\pi}{2}i - \varphi_m) < \varphi < (\frac{\pi}{2}i + \varphi_m) \end{cases} \quad (4)$$

where i = 0–3, and φ_m is the corner angle of the equilibrium shape or the first missing orientation, which was calculated as follows:

$$W(\varphi_m)\, sin\varphi_m + W_\varphi(\varphi_m)\, cos\varphi_m = 0 \quad (5)$$

$$\left(\frac{\pi}{2}i + \varphi_m\right) \le \varphi \le \left(\frac{\pi}{2}(i+1) - \varphi_m\right)(i = 0,1,2,3) \quad (6)$$

$$\tau(n)\frac{\partial \phi}{\partial t} = \nabla \cdot (W(n)^2 \nabla\phi) - \partial_x\left[W(n)W_\varphi(n)\partial_y\phi\right] + \partial_y\left[W(n)W_\varphi(n)\partial_y\phi\right] + \phi - \phi^3 - \lambda\theta(1-\phi^2)^2 \quad (7)$$

$$\left(\frac{\pi}{2}i - \varphi_m\right) < \varphi < \left(\frac{\pi}{2}i + \varphi_m\right)(i = 0,2) \quad (8)$$

$$\tau(\varphi_m)\left(\frac{cos\,\varphi}{cos\varphi_m}\right)^2 \frac{\partial \phi}{\partial t} = \tau_0(\frac{W(\varphi_m)}{cos\varphi_m})^2\phi_{xx} + \phi - \phi^3 - \lambda\theta(1-\phi^2)^2 \quad (9)$$

$$\left(\frac{\pi}{2}i - \varphi_m\right) < \varphi < \left(\frac{\pi}{2}i + \varphi_m\right)(i = 1,3), \quad (10)$$

$$\tau(\varphi_m)\left(\frac{sin\,\varphi}{cos\varphi_m}\right)\frac{\partial \phi}{\partial t} = \tau_0(\frac{W(\varphi_m)}{cos\varphi_m})^2\phi_{yy} + \phi - \phi^3 - \lambda\theta(1-\phi^2)^2 \quad (11)$$

The growth morphology of the crystals in the supercooled melts will not only be related to the crystal growth mechanism but will also have an important relationship with the solidification interface structure. The interfacial free energy will have an important influence on the interfacial structure. For weakly anisotropic crystals, the interfacial free energy in the diffusion interface region can be expressed as follows:

$$\tau(n) = \tau_0(1 + \varepsilon\, cos\, k\, \theta_i{}')^2 \quad (12)$$

$$w(n) = w_0(1 + \varepsilon\, cos\, k\, \theta_i{}') \quad (13)$$

where k is the anisotropy modulus, usually taken as 4, ε is the anisotropy coefficient, θ_i' is the angle between the preferred growth direction of a certain grain, w_0 is the length range parameter, and and τ_0 is the time length range, and this paper takes 1:

$$\theta_i{}' = f(\eta_i) + \theta \quad (14)$$

where the subscript i represents a certain grain, ϕ_y and ϕ_x represent the partial derivatives of the phase field in the x- and y- directions, respectively, and $\theta = arctan \quad (\varphi_y/\varphi_x)$ represents the angle between the interface normal and crystal growth principal axis, following

$$f(\eta_i) = r_i\pi/2(i = 1,2,\cdots,n) \tag{15}$$

where n represents the number of crystal grains, and γ_i is a random number between 0 and 1.

The temperature field governing the equation of the coupled flow field is given by [20]

$$\partial_t u + (1-\varphi)V \bullet \nabla u = D\nabla^2 u + \partial_t \varphi \tag{16}$$

$$u = (T - T_m)/(L/C_p),$$

where μ is the dimensionless temperature, T_m is the melting point temperature, L and C_p are the latent heat and specific heat respectively, V is the flow rate, and D is the thermal diffusivity, which $(1-\varphi)$ could be used to control the velocity of the solid phase to be 0.

The coupled phase field of mass conservation equation and momentum equation had the following form:

$$\nabla \bullet [(1-\varphi)V] = 0 \ , \tag{17}$$

$$\partial_t[(1-\varphi)V] + (1-\varphi)V \bullet \nabla V$$

$$= -(1-\varphi)\nabla p/\rho + \nabla \bullet [\nu\nabla(1-\varphi)V] + {M_1}^d \tag{18}$$

where ρ, p, and υ denote the density, pressure, and motion viscosity coefficient of the fluid respectively, ${M_1}^d$ is the interface dissipative force per unit volume, which can be defined as${M_1}^d = -\nu\frac{2h\varphi^2(1-\varphi)}{W_0}V$, and $(\varphi \to 1)$ to ensure that the flow rate is 0 in the solid phase, and that $(\varphi \to 0)$ attenuates in the liquid phase, where h = 2.757.

3. Determination and simulation calculations of the phase field parameters

3.1 Initial and boundary conditions

The coordinates of the crystal nuclei in the calculation grid were randomly given; thus, the crystal nuclei were randomly distributed in the simulation area. The number of crystal grains consisted of any number less than the maximum number of nuclei. The maximum number of nuclei could be calculated from the nucleation density, assuming that the variation of the nucleation density in the model satisfied a Gaussian distribution, and was given by

$$\frac{dn}{d(\Delta T)} = \frac{n_{max}}{\sqrt{2}\Delta T_\sigma} exp\left(-\frac{(\Delta T - \Delta T_{max})^2}{2{\Delta T_\sigma}^2}\right) \tag{19}$$

where ΔT_{max} is the maximum nucleation undercooling, ΔT_σ is the standard deviation of the undercooling degree, and n_{max} is the maximum nucleation density.

$$x^2 + y^2 \le R^2, \ \psi = 1, \ u = 0, \ V_x = 0, \ p = 0 \tag{20}$$

$$x^2 + y^2 > R^2, \ \psi = -1, \ u = -\Delta, \ V_x = 0, \ p = 0 \tag{21}$$

where x and y are the abscissa and ordinate, respectively, △ is the degree of undercooling, and p is the pressure. On the calculation boundary, the phase field, temperature field, and pressure used Neumann conditions.

3.2 Material physical parameters

Monocrystalline and polycrystalline silicon microstructure evolution under convection was simulated by the phase field method. The physical properties of the substance are shown in Table 1.

Table 1. Physical properties of silicon.

Property	Value
Density ρ	2570 kg/m^3
Melting point Tm	1687 K
Thermal conductivity λ	66.5 W/k·m
Kinematic viscosity μ	8 × 10−4 Pa·s
Latent heat L	1.587 × 106 J/kg

3.3 Numerical calculation method

The space step $\Delta x = \Delta y$, $\Delta x < w_0$ and the time step should satisfy

$\Delta t = 0.2 \times min\{\Delta t_1, \Delta t_2\}$,

where $\Delta t_1 = (\Delta x^2 + \Delta y^2)/2D = \Delta x^2/D$, and $\Delta t_2 = \tau_0 \Delta x^2/w_0^2$; Δt_1 is obtained from the governing equation of the temperature field, Δt_2 can be obtained from the governing equation of the phase field, and D is the thermal diffusivity. The phase field equations and the temperature field equations were solved simultaneously using explicit finite differences.

By coupling the phase field equation, mass conservation equation, momentum equation, and temperature equation, the phase field model of the coupled flow field was established, and the multi-grain, different preferred growth direction, and early and late nucleation competition growth were introduced into the model to make the model more closely resemble reality.

4. Analysis of the simulation results

4.1 Influence of undercooling degree

The degree of undercooling will play a decisive role in crystal evolution, where the smaller the supercooling, the slower the crystal growth, and the longer the growth process. With a greater degree of supercooling, the faster the crystallization process, the faster the release of latent heat of crystallization, the more the increase in temperature in the liquid at the front of the solid-liquid interface, and the greater the negative temperature gradient in the liquid, which will be more conducive to crystal growth. To visually show the effect of undercooling on the growth morphology of single crystal silicon, the undercooling values were changed in turn to simulate, U = 1.5, γ = 0.06, λ = 6.359, and D = 4, and the results are shown in Figure 1.

With a small supercooling degree, anisotropy was not obvious and the grain growth was very slow. Only the upstream side crystals were washed by the upstream supercooling solution, which led to an increase in the surrounding supercooling degree and rapid growth of dendrites. With a faster increase in the undercooling degree of the solid-liquid interface heat spread, interfacial anisotropy became more obvious, and the growth rate in the crystal axis direction gradually increased and exceeded the growth rate in the other directions. The upstream state of dendrite growth was still the fastest, the downstream was the slowest, and the morphology of dendrite growth was no longer a center of symmetry. However, the dendrite morphology was still smooth. When the supercooling degree increased above 0.65, the grain morphology was dendritic overall; however, the interface became unstable, and side branches appeared in the direction of the horizontal dendrite arms, which transformed from non-facet to facet growth. The reason was that when the supercooling degree was small, the temperature gradient at the interface was small, the growth rate was slow, the disturbance

at the interface could not be quickly amplified, and the surface tension had anti-disturbance characteristics, which could cause disturbance to disappear. With a large degree of supercooling, the growth rate was fast under a large temperature gradient, the disturbance at the interface was easily amplified, and the anti-disturbance ability of surface tension could not completely offset the effect of disturbance. Therefore, the interface was unstable and the interface morphology could easily be changed.

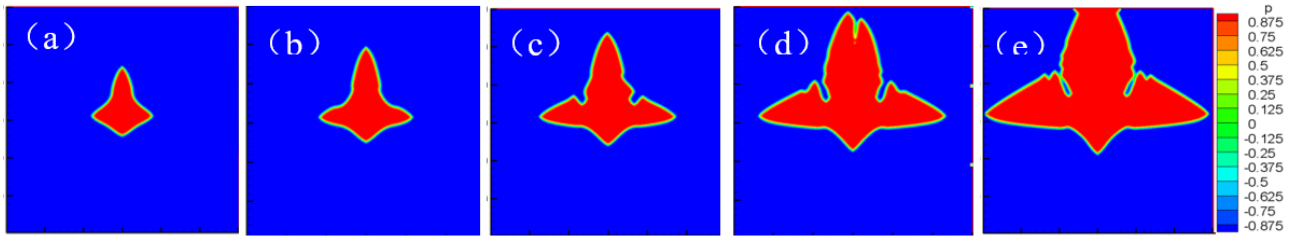

Figure. 1 △t = 30000, with undercooling of (a)△ = −0.45; (b)△ = −0.55; (c)△ = −0.65; (d)△ = −0.75; (e)△ = −0.85 crystal phase field morphology

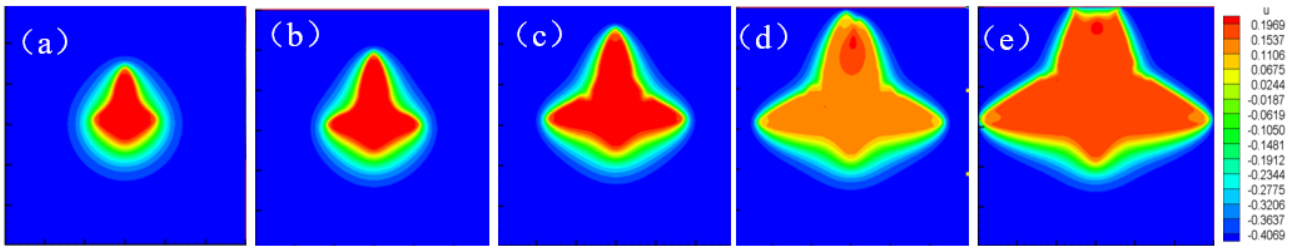

Figure. 2 △t = 30000, with undercooling of (a) △ = −0.45; (b) △ = −0.55; (c) △ = −0.65; (d) △= −0.75; (e) △ = −0.85 crystal temperature field topography

To analyze the causes of the above phenomena, the corresponding temperature field distribution was studied. Due to the influence of latent heat release during solidification, the temperature in the liquid phase was low and the temperature in the solid phase was higher. In pure diffusion theory, the smaller the degree of supercooling, the thicker the thermal diffusion layer, which could be observed by the temperature field of the downstream dendrite tip in Figure 2. Meanwhile, the upstream and horizontal directions were washed by the supercooled flowing solution, causing rapid heat diffusion, and the degree of supercooling increased, resulting in a thinner diffusion layer compared to pure diffusion theory, and crystal growth was also faster. As the degree of supercooling increased, the thermal diffusion layer became thinner, and the growth rate of the entire crystal increased.

When the degree of supercooling was small, the heat diffusion layer around the crystal was thick, which was not conducive to the release of latent heat, hindering crystal growth, and the crystal volume was small. When the supercooling degree was large, the thermal diffusion layer was thin, which was conducive to the latent heat, and its release promoted crystal growth, where the crystals that formed were larger in size. To more directly illustrate the effect of undercooling on dendrite growth, the tip velocity of the crystals under different undercooling degrees was calculated. The results are shown in Figure 3, which indicated that with an increase in supercooling, the crystal tip velocity increased linearly, which was consistent with the above analysis results.

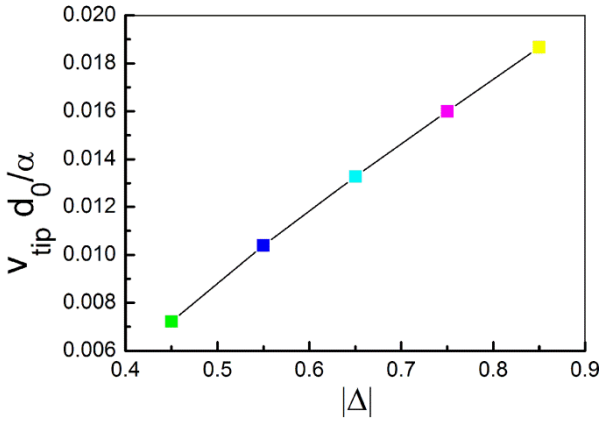

Figure. 3 Tip grid positions of the crystals at different degrees of supercooling.

The phase field parameters U = 1.5, γ = 0.06, and △ = −0.55, as well as the curve of the growth rate of each crystal tip with time, under the action of convection are shown in Figure 4. During the initial stage of solidification, the supercooling degree of each tip was very large, and the growth rate was not different. With crystal growth, a large amount of heat was released during the solidification process, which caused supercooling at the front of the crystal tip to decrease rapidly. Each crystal tip reached a different steady-state of supercooling degree over time. When the released latent heat and the convective exchange heat reached a balance, the degree of supercooling no longer changed, and the dendrites grew at a constant rate. We found that the growth rate of the upstream tip was the fastest, followed by that of the horizontal tip, and the growth rate of the downstream tip was the slowest, where the crystal growth was asymmetrical, which was consistent with the theoretical analysis results.

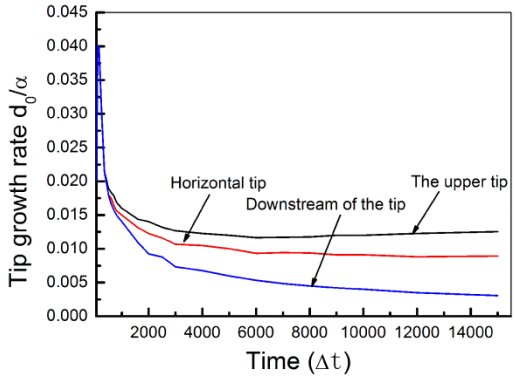

Figure. 4 Growth rate curves of each crystal tip with time under the action of convection

4.2 Effect of convection velocity on crystal morphology

Convection will play an important role in crystal growth, not only changing the crystal morphology but also greatly influencing the growth rate of each preferred crystal direction. To specifically analyze the effect of convection velocity on crystal growth, different convection velocities were considered in this study, i.e., U = 0.5, 1.0, 1.5, 2.0, and 2.5, with the same number of iterations of $t = 30000\Delta t$. The number of grids for the calculation of the phase field and temperature field of the single crystal grain was 600 × 600, the other parameters were γ = 0.06, λ = 6.359, D = 4, △x = △y = 0.4, and △ = −0.45, and the crystal morphology is shown in Figure 5. The temperature field distribution is shown in Figure 6.

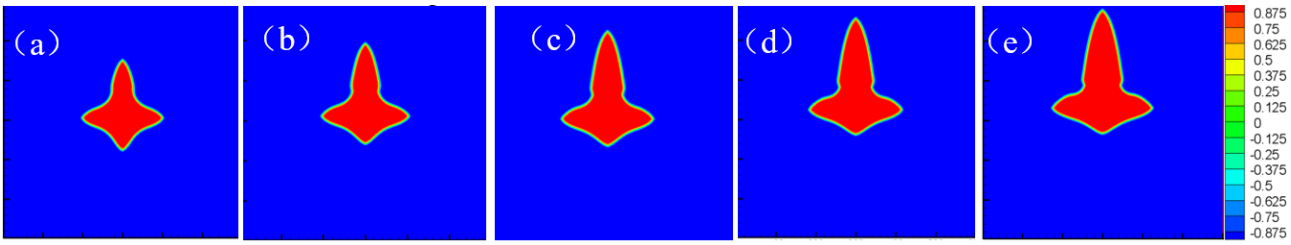

Figure. 5 t = 30000△t, with velocities of(a)U = 0.5; (b)U = 1.0; (c)U = 1.5; (d)U = 2.0; (e)U = 2.5 crystal phase field morphology.

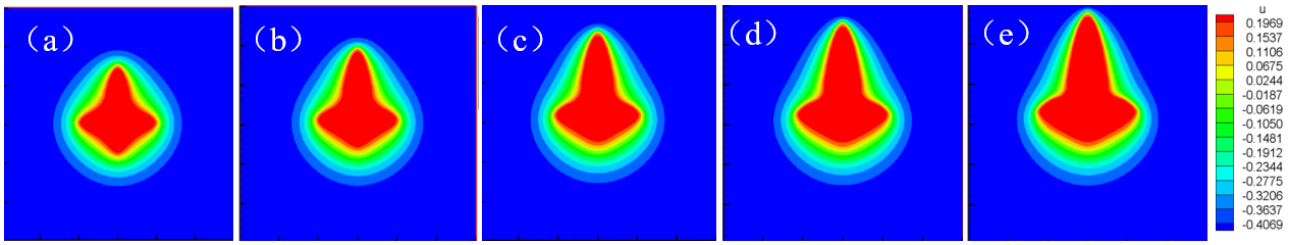

Figure. 6 t = 30000△t, with velocities of(a)U = 0.5; (b)U = 1.0; (c)U = 1.5; (d)U = 2.0; (e)U = 2.5 crystal temperature field topography.

Figure 5 shows the phase field distributions of crystal growth under the five convective velocities. As shown in the figure, the crystal growth morphology exhibited an asymmetric morphology in which the upstream dendrite growth rate was fast, while the downstream and horizontal direction growth rates were slow. In addition, the larger the added fluid velocity, the larger the entire crystal volume. At the same time, in the four preferential growth directions of the crystal nucleus, the difference in the growth rates of the dendrites in the upstream, downstream, and horizontal directions was greater, while the upstream dendrites grew the fastest. The reason could be seen in the corresponding temperature field distribution shown in Figure 6. The degree of undercooling consisted of the driving force for the solidification process. Upstream of the fluid, the temperature diffusion layer at the dendrite tip was thinner, with a large temperature gradient. In the downstream dendrite tip, the diffusion layer was thicker and the temperature gradient was smaller. Due to the scouring of the upstream dendrites by the flow of the solution, the heat released during the solidification process was removed, and the thickness of the thermal diffusion layer at the upstream dendrite tip was reduced, resulting in an increase in the actual supercooling of the upstream dendrite tip and rapid crystal growth. Downstream, a large amount of latent heat was released by the dendrites during solidification, which diffuse too late, resulting in a thick diffusion layer at the tip, a small temperature gradient, low actual undercooling, and slow growth. With an increase in the added flow rate, the scouring of the crystal tip by the supercooled fluid increased, the heat diffusion accelerated, and the diffusion layer at the tip became thinner, which led to a rapid decrease in temperature at the crystal tip and faster growth of the crystal.

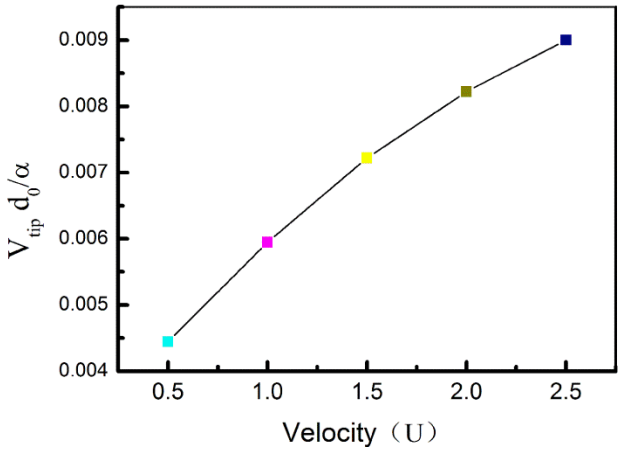

Figure. 7 Growth rate of the upstream tip at different convection

To quantitatively analyze the effect of convective velocity on crystal tip growth, we studied the change of tip growth rate with time for the different applied velocities, as shown in Figure 7. When the flow velocity increased, the steady state velocity of crystal growth also increased.

4.3 Microstructure evolution of the seed grains with different sizes and nucleation times

Based on the pure material phase field model of a single-phase system, we re-optimized the governing equation of the phase field and established the equation of interfacial free energy anisotropy that could simulate the competitive growth of multiple grains. To more accurately simulate the evolution of crystal microstructure during the initial stage of polycrystalline silicon growth, the microstructure evolution of the six seed crystals with different sizes and nucleation times was simulated under convection, where the calculated grid numbers were 1500 × 1500, $\gamma = 0.04$, $\triangle = -0.60$, and U = 1.0. The phase field is shown in Figure 8, and the temperature field is shown in Figure 9.

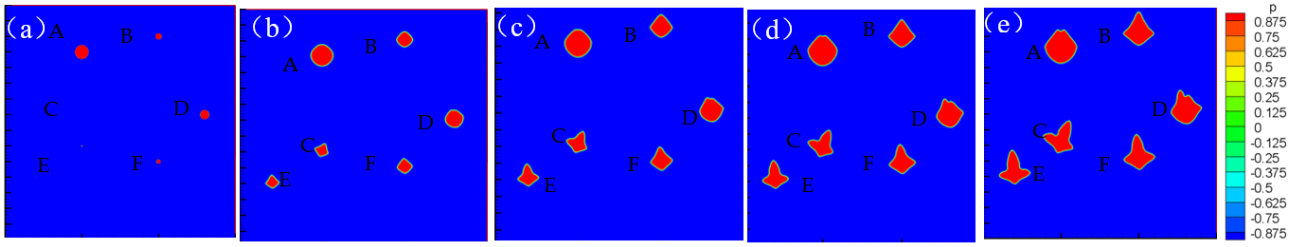

Figure. 8 Phase field images showing microstructure evolution of the polycrystals with different seed sizes and nucleation times: (a) t = 0Δt; (b) t = 3000Δt; (c) t = 6000Δt; (d) t = 9000Δt; (e) t = 12000Δt.

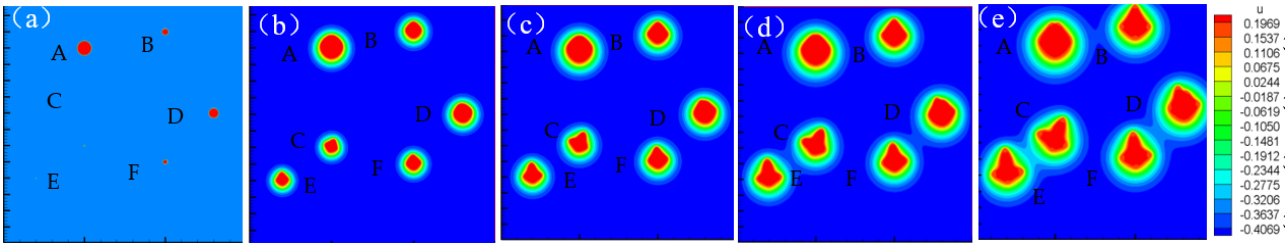

Figure. 9 Temperature field images showing polycrystal microstructure evolution with different seed sizes and nucleation times: (a) t = 0Δt; (b) t = 3000Δt; (c) t = 6000Δt; (d) t = 9000Δt; (e) t = 12000Δt.

As shown in Figure 8, the growth of each grain varied with nucleation time and the size of the nucleus under convection. The initial nucleation sizes were different, where A nucleation was the largest, C nucleation had just nucleated, and E nucleation had not yet nucleated. With prolonged simulation time, the E crystal nucleus gradually nucleated, and the other crystal nuclei grew in different preferred directions. Under the action of the flow field, the crystal showed asymmetric growth, the growth of

the upstream direction was the fastest, and the growth of the countercurrent direction was inhibited. Due to the larger radius of curvature, the asymmetric growth of A and D with larger initial nuclei was not obvious, and asymmetric growth was observed when t = 12000△t. The curvature radii of the initial nuclei B, C, E, and F were small, showing obvious asymmetric growth. With prolonged simulation time, the thermal diffusion layers of the adjacent grains made contact with each other, as shown in the temperature field images in Figure 9. The temperature gradient of grain growth decreased, which led to competitive growth among the grains, and the growth rate of the parts growing toward each other was slow.

5. Conclusions

In this work, we established a new phase field model for simulating the microstructure evolution of single crystal and polycrystalline silicon under the action of convection. The effect of phase field parameters on crystal growth was studied. The results showed that the crystal grew asymmetrically under convection. The tips grew fastest in the upstream direction, followed by those in the horizontal direction, and the bottom ends grew the slowest. The tip growth rate increased with an increase in the supercooling degree and increased with an increase in convective velocity. With different nucleation times and different nucleation sizes, each grain showed no influence on the others during the early growth stage, but the grains competed with each other in the late growth stage.

Author Contributions: Conceptualization, D.Z. and X.Y.; methodology, H.W.; software, D.Z.; validation, X.Y., D.Z. and Q.S.; formal analysis, D.Z.; investigation, X.Y.; resources, X.Y.; data curation, X.Y.; writing—original draft preparation, D.Z.; writing—review and editing, D.Z.; visualization, D.Z.; supervision, D.Z.; project administration, H.W.; funding acquisition, D.Z. All authors have read and agreed to the published version of the manuscript.

Funding

This research was funded by Youth Growth Project of Guizhou Provincial Department of Education, grant number KY (2020) 134.

Institutional Review Board Statement: Not applicable.

Informed Consent Statement: Not applicable.

Data Availability Statement: Not applicable.

Acknowledgments:

The author would like to thank the Youth Growth Project of Guizhou Provincial Department of Education, grant number KY (2020) 134, Guizhou Finance Education Fund for Postgraduate Education Reform and Quality Improvement in 2021 (No. 2021055) and the Key Laboratory of Materials Simulation and Computing of Anshun University (Asxyxkpt201803).

Conflicts of Interest: The authors declare no conflict of interest.

References

[1] Sabanskis, A.; Virbulis, J. Simulation of the influence of gas flow on melt convection and phase boundaries in FZ silicon single crystal growth. Journal of Crystal Growth, 2015, 417, 51-57.

[2] Han, X. F.; Liu, X.; Nakano ,S. et al. 3D numerical simulation of free surface shape during the crystal growth of floating zone (FZ) silicon. Journal of Crystal Growth, 2018, 483, 269-274.

[3] G. Ratnieks, A. Muiznieks, A. Muhlbauer, Modeling of phase boundaries for large industrial FZ silicon crystal growth with the needle-eye technique. Joumal of Crystal Growth, 2003, 255, 227-240.

[4] Michael , Wunscher.; Anke, Ludge.; Helge,Riemann. Growth angle and melt meniscus of the RF-heated

[5] Floating zone in silicon crystal growth. Journal of Crystal Growth, 2011, 314,43-47.

[6] P. Chen, Y.L. Tsai, C.W. Lan. Phase field modeling of growth competition of silicon grains. Acta Materialia, 2008, 56, 4114–4122.

[7] T.Aoyama, T; Kuribayshi, K. Influence of undercooling on solid/liquidinterface morphology in semiconductors . Acta Mater, 2000, 48, 3739-3744.

[8] Granasy,L.; Borzsonyi ,T.; Pusztai,T. Crystal nucleation and growth in binary phase-field theory. Phys Rev Lett, 2002, 237, 1813-1817.

[9] Granasy,L.;Borzsonyi ,T.; Pusztai ,T. Phase Field Theory of Heterogeneous Crystal Nucleation Phys Rev Lett, 2007, 98, 035703

[10] F,Wendler.; C, Mennerich.; B, Nestler. A phase-field model for polycrystalline thin film growth, J. Cryst. Growth , 2011, 327, 189-201.

[11] S,Torabi.; J, Lowengrub.; A,Voigt.;S,Wise.;A new phase-field model for strongly anisotropic systems, Proc. R. Soc. A Math. Phys. Eng. Sci, 2009, 465, 1337-1359.

[12] Kasajima,H.;Nagano,E.;Suzuki,T.Phase-field modeling for facet dendrite growth of silicon.Science and Technology of Advanced Materials, 2003, 4, 553-557.

[13] Chen,Z.; Chen,C. L.; Hao,L. M. Numerical simulation of facet dendrite growth. Transactions of Nonferrous Metals Society of China, 2008, 18, 938-943.

[14] Liu,B.Y.;Zhou,Y.Research on interface morphology evolution process of silicon materials using phase field method. Foundry Technology, 2016, 37, 2326-2330.

[15] H.K. Lin, C.W. Lan, Three-dimensional phase field modeling of silicon thin-film growth during directional solidification: facet formation and grain competition, J. Cryst. Growth, 2014, 401,740-747.

[16] S.G. Kim, W.T. Kim, Phase field modeling of dendritic growth with high anisotropy, J. Cryst. Growth, 2005, 275, 355-360.

[17] H. Kasajima, E. Nagano, T. Suzuki, S. Gyoon Kim, W. Tae Kim, Phase-field modeling for facet dendrite growth of silicon. Sci. Technol. Adv. Mater, 2003, 4,553-557.

[18] Yuan,X.F.;Yang,Y.;Liu,F.Interface morphology evolution process of solidification for multicrystalline silicon using phase-field method.Science Technology and Engineering, 2019, 19, 123-128.

[19] Du,L.F.; and Zhang, R. Phase field simulation of dendrite growth with boundary heat flux. Integrating Materials and Manufacturing Innovation, 2014, 3(1) : 1-15.

[20] Chen, G.Y. and H.K. Lin and C.W. Lan. Phase-field modeling of twin-related faceted dendrite growth of silicon. Acta Materialia, 2016, 115 : 324-332.

[21] Tong ,X.; Beckermann, C.; Karma ,A.; and Li,Q. Phase-filed Simulations of Dendritic Crystal Growth in Forced Flow. Phys Rev E, 2001, 63:061601